Red Blood Cell Thermal Fluctuations: Comparison between Experiment and Molecular Dynamics Simulations

John P. Hale,[a] Gianluca Marcelli,[b] Kim H. Parker,[c] C. Peter Winlove[a] and Peter G. Petrov*[a]

Received (in XXX, XXX) Xth XXXXXXXXX 200X, Accepted Xth XXXXXXXXX 200X
First published on the web Xth XXXXXXXXX 200X
DOI: 10.1039/b000000x

We outline a new method of analysis of thermal shape fluctuations of red blood cells, based on comparison between experiments and coarse-grained molecular dynamics simulations. The fluctuations of 2D equatorial contours of red blood cells are recorded experimentally using fast phase contrast video microscopy, from which the fluctuation spectrum is calculated. The spectrum is compared to the corresponding contour fluctuation spectrum obtained from a finite-temperature particle-dynamics simulation, modelling a cell with bending and shear elasticity and conserved volume and surface area. We demonstrate that the simulation correctly describes the mean cell shape as well as the membrane thermal fluctuations, returning physically sound values for the relevant membrane elastic moduli.

Introduction

Normal physiological function of the red blood cell (RBC) depends, amongst other factors, on finely tuned elastic properties of its plasma membrane, allowing the cell to maintain its overall shape during blood flow, yet to be flexible enough to pass through fine vessels of comparable or smaller size. Numerous experimental and theoretical studies have contributed to our understanding of the molecular and supramolecular origins of RBC elasticity. The relevant elastic parameters are the membrane bending rigidity, κ, and the membrane shear modulus, μ (assuming the membrane area to be conserved)[1]. The widely accepted current opinion is that to a first approximation, the lipid bilayer, along with its pertinent membrane proteins, controls the membrane bending elasticity whilst the membrane skeleton, mainly constructed of conjugated spectrin tetramers, endows the membrane with shear resistivity[1]. Whilst this model offers a self-consistent framework for the discussion of the RBC membrane elasticity, its experimental quantification has proved more problematic. Experimental measurements of the membrane bending modulus have led to values differing by up to an order of magnitude[2]. Similarly, the shear modulus was found, using different experimental techniques[2, 3], to range from vanishingly small up to ~10^{-5} N m^{-1}. It is possible that the discrepancies in the values obtained reflect a dependence of the membrane elastic properties on the length scale over which the deformation occurs and/or the magnitude of the applied strain. For example, analysis of the RBC thermal fluctuations[2] (i.e. at small deformations) suggest that the membrane skeleton is essentially stress free with $\mu \approx 0$, whereas the larger deformations incurred during micropipette aspiration[4] ($\mu \approx 6.6 \times 10^{-6}$ N m^{-1}), in optical tweezer experiments[5-7] ($\mu \approx 2.5 \times 10^{-6}$ N m^{-1}, $\mu \approx 3.3 \times 10^{-6}$ N m^{-1}) or in shear flow experiments[3] ($\mu \approx 10 \times 10^{-6}$ N m^{-1}) suggest higher shear stiffness. This implies a non-linear response of the membrane skeleton with respect to shear deformation. Evaluations of the bending modulus based on Brownian flicker analysis, similarly seem to suggest a separation in the values of κ depending on the length scale at which the thermal fluctuation is examined; for wavelengths smaller than the overall RBC size[8-11], $\lambda < R$, the bending rigidity is found to be of the order of 10^{-20} J, up to an order of magnitude smaller than the values obtained in the $\lambda \sim R$ regime[2, 12]. The reasons for this separation are not entirely clear, and may partly be due to the theoretical approximations used for the interpretation of the experimental fluctuation spectra.

Recent years have seen significant progress in addressing important questions such as the contribution of non-linear elasticity to RBC shapes[1], the effects of skeleton-induced tension, confinement[10] and spectrin mesh size[11] on the membrane thermal fluctuation spectrum, as well as producing diverging views on the role of ATP-dependent active membrane fluctuations[13-15]. Despite these advances, new experimental methods for quantifying erythrocyte membrane elasticity through analysis of membrane fluctuations (besides the pioneering works of Brochard and Lennon[16] and Sackmann's group[2, 8, 9, 12]) are relatively few[17, 18]. Part of the problem is that whilst the $\lambda < R$ regime is somewhat easier to analyse theoretically (using planar-membrane approximations[10]), short wavelengths are difficult to access experimentally. Long wavelengths ($\lambda \sim R$) are far easier to monitor and analyse, but the price to pay is fluctuation amplitudes affected by membrane geometry and volume and area constraints[9], which makes a purely analytical approach untenable. Recent successes in simulating quantitatively various aspects of RBC membrane behaviour such as thermal fluctuations[19], large deformations[20-22], equilibrium shapes[1], deformations in shear flow[23] etc. offer a way to circumvent such difficulties. Our approach is based on a comparison between experimentally recorded thermal fluctuation spectra and their theoretical counterparts determined from a finite-temperature particle-dynamics simulation. Since one has full control over the elasticity of the simulated mesh through the parameters of the interaction potentials, the relevant elastic constants can be evaluated by matching the fluctuation spectra. The approach is similar to that used recently simultaneously to measure the bending rigidity and effective spontaneous curvature of fluid membranes[24].

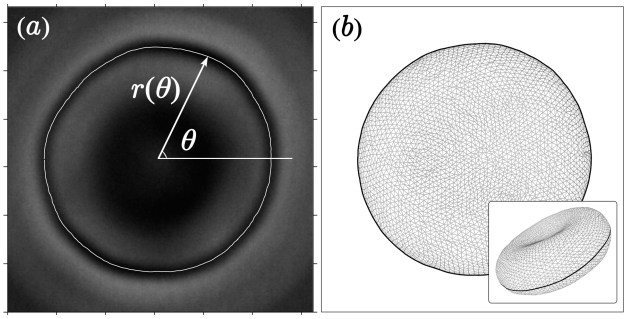

Fig. 1 (a) Snapshot of a RBC in phase contrast (diameter ~ 8 μm). The thin white line is the automatically traced 2D equatorial contour. The definition of a polar coordinate system $r(\theta)$ with an origin at the centre of area is also shown. (b) Snapshot of a simulated RBC shape. The thick black line represents the obtained 2D contour used further in the analysis of the mean square fluctuations. The inset shows a typical dyscotic shape obtained after equilibration.

Experiment

We use fast phase contrast video microscopy (Leica DMLFS upright microscope equipped with a 63× PL FLUOTAR phase contrast objective) to quantify the RBC fluctuations. The slight difference in the density between the RBCs and the surrounding buffer stabilises the cells on the bottom of the observation chamber, which allows for convenient observation of the fluctuations. 2D equatorial contours are extracted using a subpixel resolution algorithm based on the detection of the minimum intensity along the equator of the membrane (Figure 1a), with a typical frame rate of 60 fps (Moticam 2000 2 MP progressive scan digital video camera). A series of contours (between 1500 and 2500, each consisting of more than 600 points) is then analysed to quantify the membrane fluctuations. Following a standard method[24, 25], each contour is represented by a Fourier series, $r(\theta)=R\left\{1+\sum_n\left[a_n\cos(n\theta)+b_n\sin(n\theta)\right]\right\}$, where $r(\theta)$ is defined in Figure 1a. The contour shape fluctuations around the mean shape can then be quantified by the mean square values of the Fourier amplitudes for each mode n, $\left\langle\delta_n^2\right\rangle=\left[\left\langle a_n^2\right\rangle-\left\langle a_n\right\rangle^2\right]+\left[\left\langle b_n^2\right\rangle-\left\langle b_n\right\rangle^2\right]$, as in the analysis of fluctuating bilayer vesicles[26].

Figure 2 shows typical experimental fluctuation spectra. The figure shows two different cases for comparison. Case (*a*) is a cell from freshly drawn blood sample incubated in phosphate buffer (pH = 7.4) containing a small amount of albumin (1 mg ml^{-1}). To demonstrate the sensitivity of the method to changes in membrane mechanical properties, the fluctuation spectrum of the same cell, after exposure for 30 min to 0.1 mM hydrogen peroxide, is presented in (*b*). Hydrogen peroxide is known to induce the formation of haemoglobin-spectrin complexes[27, 28] resulting, amongst other changes, in decreased cell deformability and therefore we used it here as a convenient agent to stiffen the membrane.

We recorded the fluctuation spectra for several hundred fresh RBCs from healthy individuals and all of them feature the traits seen in Figure 2a. As expected, the mean square fluctuations drop for increasing mode numbers n. For intermediate values of n (between *ca.* 7 and 18) there appears

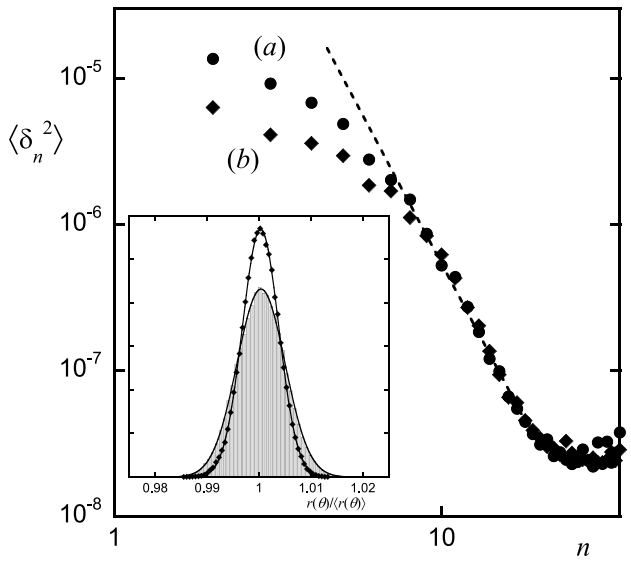

Fig. 2 Mean square fluctuations of the equatorial 2D contour, $\left\langle\delta_n^2\right\rangle$, as a function of the mode number, n, for a normal RBC (*a*), and the same cell but treated by hydrogen peroxide (*b*). Inset: normalised histogram of the fluctuations in the contour radius, $r(\theta)/\langle r(\theta)\rangle$, for the case (*a*) (bars) and (*b*) (diamonds), fitted by a normal distribution function (solid lines).

to be a power-law dependence (see the dashed line in Figure 2). Analysis of 141 fluctuating cells showed that for this part of the dependence, $\left\langle\delta_n^2\right\rangle\propto n^{-(3.95\pm0.36)}$, which suggests that this part of the fluctuation spectrum is dominated by bending. For lower mode numbers ($n \le 6$) the mean square amplitudes deviate progressively from this scaling. This deviation originates from the closed topology of the membrane and has already been comprehensively analysed for the long-wavelength modes of lipid vesicles[25]. In addition, this part of the spectrum could be affected by constraints reflecting the composite nature of the RBC membrane (i.e. a lipid bilayer coupled to a spectrin mesh) through skeleton-induced membrane tension and, importantly, suppression of bilayer fluctuations due to the confining effect of the membrane skeleton[10] (which, in turn, is related to its shear modulus, μ); the latter is expected to have a stronger effect on the longest wavelength modes[10]. Figure 2b is an illustration of these effects. Here, the addition of hydrogen peroxide increases membrane rigidity most probably through haemoglobin-spectrin cross-linking[27, 28] and possibly aggregation of band 3[29]. Thus, the membrane seems to be developing increased tension and/or shear resistance, which affects the longest-wavelength modes ($n \le 6$), whilst the bending rigidity of the lipid bilayer is not necessarily significantly altered.

The inset in Figure 2 shows a normalised histogram of the fluctuations in the instantaneous radius of the contour, $r(\theta)/\langle r(\theta)\rangle$, calculated over all contours in the sample for 360 values of the polar angle θ. It demonstrates that the radius fluctuations are normally distributed. Since this is a very sensitive measure of the overall degree of fluctuations, it can be used to detect changes in membrane stiffness, as illustrated by the comparison between cases (*a*) and (*b*).

The ability to detect short wavelength fluctuations using

this optical method is fundamentally limited by the optical resolution, camera noise and fluctuation lifetimes of the short-lived high frequencies[25] (the fluctuation lifetime for the bending-dominated part of the spectrum scales with the cube of the wavelength, $\tau_n \sim \eta\lambda_n^3/\kappa$, where η is the viscosity of the surrounding fluid[16]). We found that fast short wavelength modes, $n \geq 18$, cannot be detected reliably.

Simulation

We used a coarse-grained particle dynamics simulation to investigate the thermal fluctuations of a 2D network (embedded in a 3D closed surface) consisting of 5762 particles arranged in a regular triangulation. The bases of the method are presented in detail elsewhere[19], but in addition to the global surface area constraint, we implemented also a volume constraints, better to reflect the experimental situation. This allowed us to keep a constant volume-to-area ratio, $v = 3V/(4\pi R_A^3)$, where V is the cell volume and R_A is the equivalent radius, calculated from the cell surface area[24], $R_A = (A/4\pi)^{1/2}$. In accordance with the experimental values for the RBC volume and surface area[1], we used v = 0.65 throughout the simulations. Each pair of neighbouring particles (i,j) is allowed to interact with a harmonic potential $V_{ij}^s = (k_s/2)[(r_i - r_j) - r_0]^2$, where k_s is the spring constant (equal for all interactions), $r_{i,j}$ is the particle position and r_0 = 100 nm is the equilibrium distance between two connected particles. In addition, a dihedral angle potential is applied between each two adjacent triangles, of the form $V_{ij}^d = D(1 - \mathbf{n}_\alpha \cdot \mathbf{n}_\beta)$, where D is the relevant dihedral constant and $\mathbf{n}_{\alpha,\beta}$ is the unit normal vector of each triangle. The area constraint is implemented using Lagrange's method of undetermined multipliers. The volume is kept constant by applying an external pressure to the cell surface. The pressure is applied outwards when the volume exceeds the desired value and inwards in the opposite case. The choice of interaction potentials, along with the constant area constraint, endows the 2D mesh with finite bending and shear moduli whilst making it effectively incompressible. In order to incorporate effects from the surrounding environment, a Nosé-Hoover thermostat[30, 31] is employed to keep a constant temperature. The thermostat mimics the exchange of energy between the simulated cell and the environment. Viscous effects are not taken into account, as (according to the fluctuation-dissipation theorem) they cannot affect the equilibrium fluctuation spectrum. The system is allowed to evolve towards equilibrium and the equations of motion for the virtual particles are solved using the molecular-dynamics technique[30, 31].

We find that after an equilibration phase, the number of steps for which depends on the initial shape chosen, the simulation reaches a constant temperature and the cell model steadies into a fluctuating discocyte, thus correctly approximating the mean shape of real RBCs (a snapshot is shown in the inset of Figure 1b). The equilibrium part of the simulation can then be used to analyse the thermal shape fluctuations of the mesh. In order to correctly compare the mesh fluctuations to those of the experimental RBCs, 2D equatorial contours are obtained by intersecting the shape with a plane passing through the centre of mass (see the black solid line in Figure 1b). This procedure results in contours typically consisting of ~300 points each. Once extracted, we use about 300 contours at a time to calculate the fluctuation spectrum of

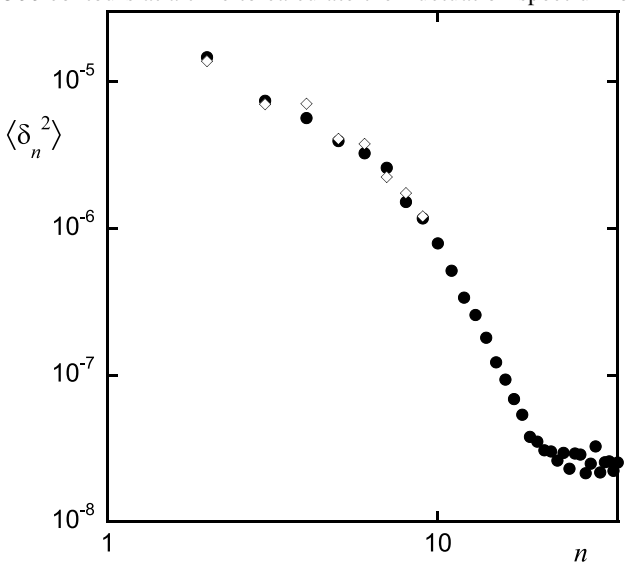

Fig. 3 Mean square fluctuations of the equatorial 2D contour, $\langle \delta_n^2 \rangle$, as a function of the mode number, n, for a normal RBC (solid circles) and a matched simulation (diamonds). Values of the interaction parameters: k_s = 8.3×10^{-6} N m^{-1} and $D = 1.3 \times 10^{-18}$ J.

the simulated contours, $\langle \delta_n^2 \rangle$, in exactly the same way as for the experimental contour sets. This allows a direct comparison of the contour shape fluctuations obtained experimentally and computationally. We generally found that for the limited number of contour points in the simulation, modes up to $n \approx$ 10 can reliably be obtained.

Comparison between simulation and experiment

Comparison between experimentally and computationally obtained fluctuation spectra shows that they are in agreement for values of the spring constant $k_s \sim 5 \times 10^{-6}$ N m^{-1} and the dihedral constant $D \sim 10^{-18}$ J. This allows an order of magnitude estimation of the (zero-temperature) shear and bending moduli using the approximate relationships reported in the literature[32, 33], $\mu \approx (\sqrt{3}/4)k_s$ and $\kappa = D/\sqrt{3}$. We obtain $\mu \sim 2 \times 10^{-6}$ N m^{-1} and $\kappa \sim 6 \times 10^{-19}$ J.

We stress that the external pressure acting as a volume constraint in the model does not affect the shear modulus as calculated by the equation above. The external pressure could give rise to membrane tension only via changes in the density of the membrane (as compared to the stress-free state), which in our model is prevented by the area constraint. We also established that trere was no correlation between the temporal behaviour of the applied pressure and that of the fluctuation modes, which means that the fluctuation modes (and therefore the membrane bending modulus) are not affected by the external pressure.

Figure 3 shows an example of a direct comparison between

an experimentally obtained fluctuation spectrum of a normal RBC and its simulation counterpart. The values of the interaction potential constants are $k_s = 8.3 \times 10^{-6}$ N m^{-1} and $D = 1.3 \times 10^{-18}$ J, giving a shear modulus $\mu \approx 3.6 \times 10^{-6}$ N m^{-1} and a bending modulus $\kappa \approx 7.5 \times 10^{-19}$ J.

The value for the bending modulus compares favourably with previous experiments in the same wavelength regime ($\lambda \sim R$)[2, 12]. For example, the theoretical interpretation performed by Peterson et al.[12] for RBC thickness fluctuations suggest a bending modulus of $(1.4 - 4.3) \times 10^{-19}$ J, depending on the elastic model used. Strey et al.[2] analysed RBC membrane flicker at four orthogonal points around the membrane at wavelengths comparable to the cell dimensions. For the bending modulus they obtained a mean value of 4×10^{-19} J, with individual measurements covering the range from 2×10^{-19} J to 7×10^{-19} J.

Whilst the values obtained for the membrane bending rigidity are of the same order of magnitude as those reported in previous studies of the long-wavelength regime, the shear modulus obtained, 3.6×10^{-6} N m^{-1}, is closer to the values reported in static deformation experiments, such as micropipette aspiration[4] and optical tweezers studies[5-7]. This seems to contradict previous conclusions[2] that freely flickering RBCs, i.e. at small shear deformations, have negligible (less than ~10^{-7} N m^{-1}) shear modulus. Our results support the notion that the RBC membrane skeleton may not necessarily show vanishingly small shear rigidity at small deformations. Further evidence for this conclusion could be drawn from previous Monte Carlo polymer chain simulations of the erythrocyte cytoskeleton[34] which suggest a shear modulus as high as ~10^{-5} N m^{-1}. It is interesting to note that recent models of the RBC membrane that explicitly consider its composite nature lead to similar conclusions. For example, Gov et al.[10] take into account the influence of the spectrin network through two parameters in the free energy functional, an effective surface tension, σ, and a confining parameter, γ, both related to the stiffness of the spectrin filaments. The confining parameter γ, which serves to constraint the bilayer fluctuations due to the proximity of the (rigid) membrane skeleton, can be seen to depend on the bending and shear membrane moduli[10], $\gamma \approx \mu^2/\kappa$. Analysing experimental short-wavelength fluctuation data[8] for two RBCs, these authors find $\gamma = 1.0 \times 10^7$ J m^{-4} and $\gamma = 7.5 \times 10^7$ J m^{-4}. This, in turn, suggests that the skeleton shear modulus could reach a value of the order of 10^{-6} N m^{-1} even when a small value of $\kappa \approx 2 \times 10^{-20}$ J, characteristic for the short wavelength regime, is used.

Conclusions

We demonstrated the feasibility for interpretation of the long-wavelength part of the RBC membrane fluctuation spectrum through a coarse-grained particle dynamics simulation. The simulation faithfully reproduces the average cell dyscotic shapes and correctly describes the mean square fluctuations of the equatorial contours of RBCs, returning physically meaningful values for the elastic membrane parameters. Further work is underway in our laboratories exploring comprehensively the parameter space of the simulation through variations in the values of the interaction potential parameters, volume to area ratio and the size of the simulated mesh, which will allow fast quantification of the elastic constants of any RBC.

Acknowledgements

We enjoyed fruitful discussions with H.-G. Döbereiner, N. Mohandas, J. Evans, J. Sleep, W. Gratzer and P. Cicuta. This work was partly supported by the University of Exeter Reasearch Fund.

Notes and references

[a] *School of Physics, University of Exeter, Stocker Road, Exeter EX4 4QL, UK. E-mail: p.g.petrov@exeter.ac.uk*
[b] *Division of Engineering, King's College London, Strand Campus, London WC2R 2LS, UK.*
[c] *Department of Bioengineering, Imperial College London, Exhibition Road, London SW7 2AZ, UK.*

1. H. W. G. Lim, M. Wortis and R. Mukhopadhyay, *Proc. Natl. Acad. Sci. U. S. A.*, 2002, **99**, 16766-16769.
2. H. Strey, M. Peterson and E. Sackmann, *Biophys. J.*, 1995, **69**, 478-488.
3. R. M. Hochmuth, N. Mohandas and P. L. Blackshear, *Biophys. J.*, 1973, **13**, 747-762.
4. R. Waugh and E. A. Evans, *Biophys. J.*, 1979, **26**, 115-131.
5. S. Hénon, G. Lenormand, A. Richert and F. Gallet, *Biophys. J.*, 1999, **76**, 1145-1151.
6. M. Dao, C. T. Lim and S. Suresh, *J. Mech. Phys. Solids*, 2003, **51**, 2259-2280.
7. M. Dao, C. T. Lim and S. Suresh, *J. Mech. Phys. Solids*, 2005, **53**, 493-494.
8. A. Zilker, H. Engelhardt and E. Sackmann, *J. Phys.*, 1987, **48**, 2139-2151.
9. A. Zilker, M. Ziegler and E. Sackmann, *Phys. Rev. A*, 1992, **46**, 7998-8001.
10. N. Gov, A. G. Zilman and S. Safran, *Phys. Rev. Lett.*, 2003, **90**, 228101.
11. J. B. Fournier, D. Lacoste and E. Raphaël, *Phys. Rev. Lett.*, 2004, **92**, 018102.
12. M. A. Peterson, H. Strey and E. Sackmann, *J. Phys. II*, 1992, **2**, 1273-1285.
13. S. Levin and R. Korenstein, *Biophys. J.*, 1991, **60**, 733-737.
14. S. Tuvia, S. Levin, A. Bitler and R. Korenstein, *J. Cell Biol.*, 1998, **141**, 1551-1561.
15. J. Evans, W. Gratzer, N. Mohandas, K. Parker and J. Sleep, *Biophys. J.*, 2008, **94**, 4134-4144.
16. F. Brochard and J. F. Lennon, *J. Phys.*, 1975, **36**, 1035-1047.
17. L. G. Mesquita, U. Agero and O. N. Mesquita, *Appl. Phys. Lett.*, 2006, **88**, 133901.
18. G. Popescu, T. Ikeda, K. Goda, C. A. Best-Popescu, M. Laposata, S. Manley, R. R. Dasari, K. Badizadegan and M. S. Feld, *Phys. Rev. Lett.*, 2006, **97**, 218101.
19. G. Marcelli, K. H. Parker and C. P. Winlove, *Biophys. J.*, 2005, **89**, 2473-2480.
20. D. E. Discher, D. H. Boal and S. K. Boey, *Biophys. J.*, 1998, **75**, 1584-1597.
21. J. Li, M. Dao, C. T. Lim and S. Suresh, *Biophys. J.*, 2005, **88**, 3707-3719.
22. I. V. Pivkin and G. E. Karniadakis, *Phys. Rev. Lett.*, 2008, **101**, 118105.
23. H. Noguchi and G. Gompper, *Proc. Natl. Acad. Sci. U. S. A.*, 2005, **102**, 14159-14164.
24. H.-G. Döbereiner, G. Gompper, C. K. Haluska, D. M. Kroll, P. G. Petrov and K. A. Riske, *Phys. Rev. Lett.*, 2003, **91**, 048301.

25. J. Pécréaux, H.-G. Döbereiner, J. Prost, J. F. Joanny and P. Bassereau, *Eur. Phys. J. E*, 2004, **13**, 277-290.
26. H. P. Duwe, J. Kaes and E. Sackmann, *J. Phys.*, 1990, **51**, 945-961.
27. L. M. Snyder, N. L. Fortier, J. Trainor, J. Jacobs, L. Leb, B. Lubin, D. Chiu, S. Shohet and N. Mohandas, *J. Clin. Invest.*, 1985, **76**, 1971-1977.
28. C. R. Kiefer, J. F. Trainor, J. B. McKenney, C. R. Valeri and L. M. Snyder, *Blood*, 1995, **86**, 366-371.
29. P. S. Low, S. M. Waugh, K. Zinke and D. Drenckhahn, *Science*, 1985, **227**, 531-533.
30. M. P. Allen and D. J. Tildesley, *Computer Simulation of Liquids*, Clarendon Press, Oxford, 1987.
31. R. J. Sadus, *Molecular Simulation of Fluids: Theory, Algorithms and Object-Orientation*, Elsevier Press, Amsterdam, 1999.
32. D. E. Discher, D. H. Boal and S. K. Boey, *Phys. Rev. E*, 1997, **55**, 4762-4772.
33. G. Gompper and D. M. Kroll, *J. Phys. I*, 1996, **6**, 1305-1320.
34. D. H. Boal, *Biophys. J.*, 1994, **67**, 521-529.

Red Blood Cell Thermal Fluctuations: Comparison between Experiment and Molecular Dynamics Simulations

John P. Hale, Gianluca Marcelli, Kim H. Parker, C. Peter Winlove and Peter G. Petrov*

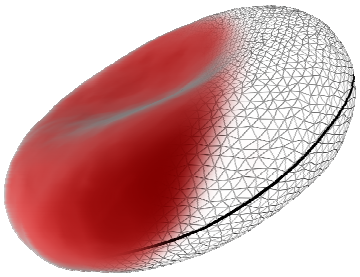

A new method of analysis of thermal shape fluctuations of red blood cells, based on comparison between experiments and coarse-grained molecular dynamics simulations, is reported. It allows the direct quantification of the membrane shear and bending elasticity.